Erratum

Nakano, I., Kobayashi, T., Yoshimura, M. and Shingyoji, C. (2003). Central-pair-linked regulation of microtubule sliding by calcium in flagellar axonemes. *J. Cell Sci.* **116**, 1627-1636.

We apologise for two errors in Fig. 1. In Fig. 1A and Fig. 1C the concentration of ATP should be 20 μM not 20 M. The correct figure is shown below.

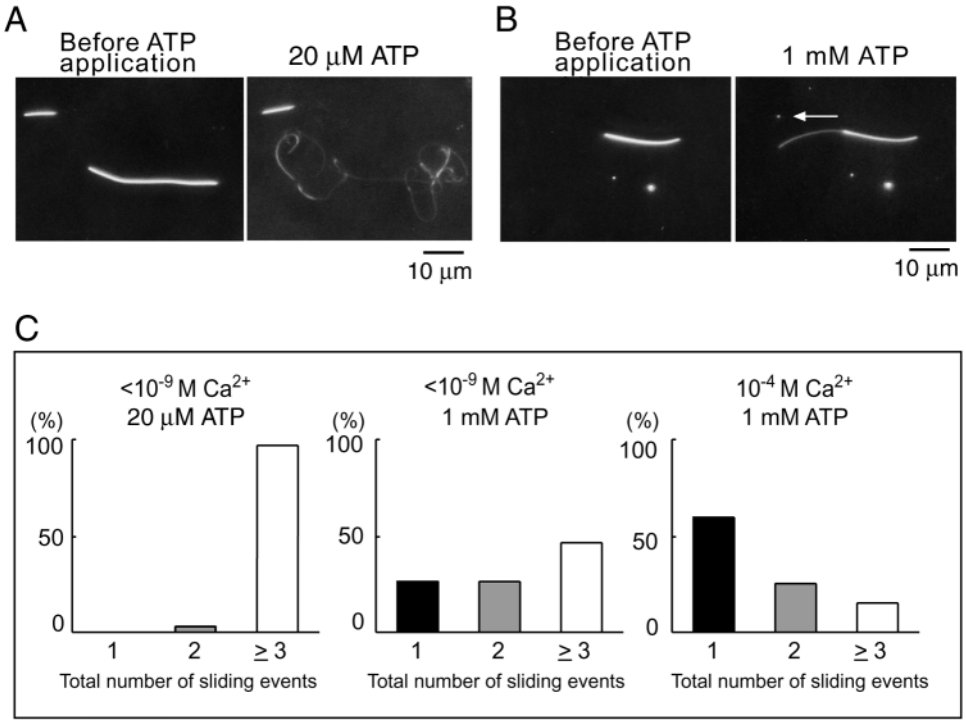

Central-pair-linked regulation of microtubule sliding by calcium in flagellar axonemes

Izumi Nakano, Takeshi Kobayashi*, Misako Yoshimura and Chikako Shingyoji‡

Department of Biological Sciences, Graduate School of Science, University of Tokyo, Hongo, Tokyo 113-0033, Japan

*Present address: ERATO Kusumi Membrane Organizer Project, JST, Kumazaki bldg. 5-11-33 Chiyoda, Naka-Ku, Nagoya 460-0012, Japan

‡Author for correspondence (e-mail: chikako@biol.s.u-tokyo.ac.jp)

Accepted 21 December 2002

Journal of Cell Science 116, 1627-1636 © 2003 The Company of Biologists Ltd

doi:10.1242/jcs.00336

Summary

The movement of eukaryotic flagella and cilia is regulated by intracellular calcium. We have tested a model in which the central pair of microtubules mediate the effect of Ca^{2+} to modify the dynein activity. We used a novel microtubule sliding assay that allowed us to test the effect of Ca^{2+} in the presence or absence of the central-pair microtubules. When flagellar axonemes of sea-urchin sperm were exposed to ATP in the presence of elastase, they showed different types of sliding disintegration depending on the ATP concentration: at low concentrations of ATP (≤50 μM), all the axonemes were disintegrated into individual doublets by microtubule sliding; by contrast, at high ATP concentrations (≥100 μM), a large proportion of the axonemes showed limited sliding and split lengthwise into a pair of two microtubule bundles, one of which was thicker than the other. The sliding behaviour of the axonemes was also influenced by Ca^{2+}. Thus, at 1 mM ATP, the proportion of axonemes that split into two bundles increased from 25% at <10^{-9} M Ca^{2+} to 60% at 10^{-4} M Ca^{2+}, whereas the sliding velocity of doublets during the splitting did not change. Electron microscopy of split bundles showed that the thicker bundles contained five or six doublets and the central pair, whereas the thinner bundles contained three or four doublets but not the central pair. Closer examinations revealed that the thicker bundles were dominated by four patterns of doublet combinations: doublets 8-9-1-2-3-4, 8-9-1-2-3, 4-5-6-7-8 and 3-4-5-6-7-8. This indicates that the sliding occurred preferentially at one or two fixed interdoublet sites on either side of the central-pair microtubules, whereas the sliding at the remaining interdoublet sites was inhibited under these conditions. Ca^{2+} reduced the appearance of the 4-5-6-7-8 and 3-4-5-6-7-8 patterns and increased the 8-9-1-2-3-4 and 8-9-1-2-3 patterns. The splitting patterns are possibly related to the switching mechanism of the dynein activity underlying the cyclical flagellar bending. To investigate the role of the central pair in the regulation of the dynein activity by Ca^{2+}, we studied the behaviour of singlet microtubules applied to the dynein arms exposed on the doublets of the split bundles that were either associated with the central pair or not. Microtubules moved along both the thicker and the thinner bundles but the frequency of microtubule sliding on the thinner (i.e. the central-pair-less) bundles was three to four times (at ≤10^{-5} M Ca^{2+}) and ten times (at 10^{-4} M Ca^{2+}) as large as that on the thicker, central-pair-associated bundles. Furthermore, the velocity of microtubule sliding at 1 mM ATP on the thicker bundles were significantly reduced by 10^{-7}-10^{-4} M Ca^{2+}, whereas that on the thinner bundles was not changed by the concentration of Ca^{2+}. These results indicate that Ca^{2+} inhibits the activity of dynein arms on the doublets through a regulatory mechanism that involves the central pair and the radial spoke complex. This mechanism might control the switching of the dynein activity within the axoneme to induce the oscillatory bending movement of the flagellum.

Key words: Dynein, Sliding velocity, Sliding pattern, 9+2 structure, Elastase

Introduction

Our goal is to determine the mechanism by which Ca^{2+} regulates flagellar motility. Changes in the intracellular concentration of Ca^{2+} have profound effects on the bending patterns of cilia and flagella (Naitoh and Kaneko, 1972; Izumi and Miki-Noumura, 1985; Holwill and McGregor, 1976). In *Chlamydomonas* flagella, an increase in the intracellular Ca^{2+} changes the flagellar waveform from an asymmetrical ciliary type to a symmetrical flagellar type (Hyams and Borisy, 1978; Bessen et al., 1980; Omoto and Brokaw, 1985). In sea urchin sperm flagella, Ca^{2+} increases the asymmetry of waveform, ultimately inducing a stoppage (‘quiescence’) of flagellar beating above 10^{-4} M Ca^{2+} (Brokaw, 1979; Gibbons and Gibbons, 1980). It is likely that the effect of Ca^{2+} on the flagellar movement is related to the regulation of microtubule sliding, but the mechanism of regulation by Ca^{2+} has been poorly understood.

The central pair of microtubules (central apparatus) and the radial spokes are thought to form a complex (CP/RS) that regulates the activity of dynein arms. The rotation of the central pair during ciliary and flagellar beating suggests that the central pair might act as a ‘distributor’ to regulate the activity of dynein arms (Omoto et al., 1999). The CP/RS is also implicated in the Ca^{2+}-dependent conversion of the waveforms. In *Chlamydomonas*, the flagella of mutants lacking the CP/RS do not beat, even though their axonemes are capable of sliding disintegration (Witman et al., 1978; Kamiya, 2002). At low ATP concentrations (<20 μM), however, the CP/RS-deficient

axonemes are capable of beating and, in response to Ca^{2+}, convert the waveform from an asymmetrical (at $<10^{-6}$ M Ca^{2+}) to a symmetrical (at $\geq 10^{-5}$ M Ca^{2+}) pattern, although they are non-beating at high ATP concentrations (Wakabayashi et al., 1997). At physiological concentrations of ATP (~1 mM), the central-pair microtubules are probably involved in the response to Ca^{2+} in the wild type (Hosokawa and Miki-Noumura, 1987) as well as in the CP/RS mutants of *Chlamydomonas* (Smith, 2002b). The ATP-dependent role of the CP/RS in the Ca^{2+} regulation is also observed in sea urchin sperm flagella. Based on the analysis of flagellar waveforms of flagella 'beating' under imposed head vibration (Gibbons et al., 1987), we showed that Ca^{2+} decreased the velocity of microtubule sliding through a trypsin-sensitive regulatory mechanism, which possibly involves the central-pair microtubules (Bannai et al., 2000). This was also supported by the artificially induced rotation of the Ca^{2+}-induced asymmetrical bending pattern. The rotation of the beating plane under imposed head vibration occurred only at high ATP concentrations (≥100 μM), indicating that the regulation of dynein activity through the central pair occurs only at high ATP concentrations (Bannai et al., 2000). These studies suggest that, at least at ATP concentrations higher than ~100 μM, high concentrations of Ca^{2+} modify the regulatory signal from the central pair, which is mediated by the radial spokes to control the activity of the dynein arms.

In this study, we tested the idea that Ca^{2+} alters the dynein activity, using a novel microtubule sliding assay. As the protease necessary to initiate sliding between the doublets, we used elastase (Brokaw, 1980) instead of trypsin, although trypsin is more widely used, to digest axonemal structures that restrict free sliding of the doublets (Summers and Gibbons, 1971). Unlike the trypsin-treated axonemes, which do not show oscillatory bending movements in response to local, repetitive application of ATP, the elastase-treated axonemes were capable of oscillatory bending movements, indicating that they retained certain regulatory mechanisms for producing local cyclical bending (Shingyoji and Takahashi, 1995).

When the elastase-treated axonemes were exposed to physiological concentrations (e.g. 1 mM) of ATP, they split lengthwise into two unequal microtubule bundles: a thicker bundle that contained the central-pair microtubules and a thinner one that did not. We found that 10^{-4} M Ca^{2+} did not affect the velocity at which the two bundles slid along each other during the splitting, although it affected the patterns into which the axonemes split. Electron microscopic analysis of the split bundles showed that the axonemes were split into a pair of bundles at some preferred interdoublet sites that were close to either of the central pair.

To study the effect of the central pair on the dynein activity at high Ca^{2+}, we used the microtubule sliding assay developed by Yoshimura and Shingyoji (Yoshimura and Shingyoji, 1999), which was a modification of the method of Shingyoji et al. (Shingyoji et al., 1998). In the present study, we analysed the behaviour of singlet microtubules that were made to interact with either the thicker or the thinner bundles obtained from the splitting of the axonemes. We found that the velocity of microtubule sliding on the thicker bundles, which contained the central-pair microtubules, was significantly decreased by 10^{-7}-10^{-4} M Ca^{2+}. The frequency of microtubule sliding on the bundles was significantly reduced by the presence of the central pair but was not affected by Ca^{2+} except at 10^{-4} M. These results indicate that Ca^{2+} alters the sliding activity of dynein arms in flagella through the CP/RS complex.

Materials and Methods

Axonemes and microtubules

Sperm of the sea urchins *Pseudocentrotus depressus* and *Clypeaster japonicus* were suspended in the same volume of Ca^{2+}-free artificial sea water (465 mM NaCl, 10 mM KCl, 25 mM $MgSO_4$, 25 mM $MgCl_2$ and 2 mM Tris-HCl, pH 8.0) and demembranated with 15 volumes of demembranating solution [0.04% (w/v) Triton X-100, 0.15 M potassium acetate, 2 mM $MgSO_4$, 2 mM glycoletherdiamine-*N*,*N*,*N*′,*N*′-tetra-acetic acid (EGTA), 1 mM dithiothreitol (DTT), 10 mM Tris-HCl, pH 8.0] for 45 seconds at 20-23°C (*Pseudocentrotus*) or 24-27°C (*Clypeaster*). The demembranated sperm suspension was diluted with 16 volumes of reactivating solution [0.15 M potassium acetate, 2 mM $MgSO_4$, 2 mM EGTA, 1 mM DTT, 2% (w/v) polyethyleneglycol (MW 20,000) and 10 mM Tris-HCl, pH 8.0] without ATP. For *Clypeaster* (in the new sliding assay experiment), 20 mM HEPES (pH 7.8) was used instead of Tris (pH 8.0) in both demembranating and reactivating solutions. Preparations that showed less than 90% reactivation at 1 mM ATP were discarded.

The demembranated sperm were fragmented by passing a sperm suspension through a 22-gauge hypodermic needle (for sliding disintegration experiments and electron microscopy) or by homogenizing the sperm suspension (for new sliding assay experiments). Sperm heads were removed by centrifugation at 2,000-4000 ***g***; the supernatant containing axonemal fragments was centrifuged at 17,000-20,000 ***g*** and resuspended in reactivating solution (without ATP). For observation of the sliding at 1 mM ATP (0.6-0.9 mM MgATP) and 10^{-4} M Ca^{2+}, ATP and $CaCl_2$ were added to the reactivating solution following calculations according to Goldstein (Goldstein, 1979).

For the new sliding assay experiments, demembranated sperm were labelled with tetramethylrhodamine before fragmentation, and singlet microtubules were assembled from tetramethylrhodamine-labelled bovine tubulin according to Yoshimura and Shingyoji (Yoshimura and Shingyoji, 1999). Strongly labelled singlet microtubules were distinguished from weakly labelled fragmented axonemes by adjusting the illumination.

Observation of sliding disintegration and microtubule sliding

Sliding disintegration of doublet microtubules was observed by the method described by Takahashi et al. (Takahashi et al., 1982). The axonemal fragments in ATP-free reactivating solutions containing or not containing $CaCl_2$ were first placed between two coverslips separated by two strips of plastic adhesive tape used as spacers, thus forming a chamber that was open on two sides. They were then perfused with the reactivating solution containing the same concentration of $CaCl_2$ and 20 μM or 1 mM ATP. Finally, they were perfused with a reactivating solution containing elastase (5 μg ml^{-1} elastase, Sigma type III and 5 μg ml^{-1} trypsin inhibitor, Sigma type I-S) as well as the same concentrations of $CaCl_2$ and ATP.

Observation was made using an inverted microscope (Nikon, TMD) fitted with a 40× objective lens (Nikon), a dark-field condenser (Nikon, NA=0.95-0.80), heat-absorbing filters and a halogen lamp. Sliding disintegration was recorded on videotape using a CCD camera (Hamamatsu Photonics, C2400-77) and a U-matic videocassette recorder (Sony, VO-5800), enhancing the contrast of the image with a control unit (Hamamatsu Photonics, ARGUS-10) and a CCD camera unit (Hamamatsu Photonics, C2400). To analyse the sliding velocity, the recorded images were imported into a personal computer by using LF-3 Scientific Frame Grabber (Scion Corporation) and the displacement of the doublet microtubule was measured by using the

NIH Image software. The sliding velocity was determined by plotting the displacement against time and applying the least-squares method to the plots.

For the observation of microtubule sliding on the doublet bundles in the new sliding assay experiment, we first induced sliding disintegration of elastase-treated rhodamine-labelled axonemes by the same procedure as used in the previous study (Yoshimura and Shingyoji, 1999), except for the following: the two sides of the slide of the 5 μl chamber were sealed with adhesive plastic tape instead of enamel in order to obtain a constant depth of the perfusion solution. A suspension of axonemal fragments was first introduced into the chamber and treated with elastase (5 μg ml^{-1} elastase, Sigma type III and 5 μg ml^{-1} trypsin inhibitor, Sigma type I-S, in the reactivating solution containing 10^{-4} M Ca^{2+} without ATP) for 1-1.5 minutes. The elastase treatment was stopped with ovoinhibitor (50 μg ml^{-1} ovoinhibitor, Sigma type IV-O, in reactivating solution containing 10^{-4} M Ca^{2+} without ATP), and followed by perfusion with casein (~1 mg ml^{-1} in reactivating solution containing 10^{-4} M Ca^{2+} without ATP). The perfusion of reactivating solution containing 10^{-4} M Ca^{2+} and 1 mM ATP (0.6 mM MgATP) then induced sliding disintegration of the axonemal fragments into two parts. As the next step, to reduce the Ca^{2+} concentration, the assay buffer (see below) without EGTA was perfused followed by perfusion of the assay buffer containing 1 mM ATP (0.9 mM MgATP) with or without Ca^{2+}. The rhodamine-labelled microtubules were suspended in the assay buffer to which 2% (v/v) β-mercaptoethanol, 40 mM glucose, 430 μg ml^{-1} glucose oxidase, 70 μg ml^{-1} catalase, 10 μM Taxol and the same concentration of MgATP and Ca^{2+} had been added. The assay buffer contained 70 mM potassium acetate, 5 mM magnesium acetate, 20 mM HEPES, 2 mM EGTA, 0.1 mM ethylenediaminetetraacetic acid (EDTA) and 1 mM DTT, pH 7.8. The concentrations of Ca^{2+} in the solution used for the observation of microtubule sliding were $<10^{-9}$ M, 10^{-7} M, 10^{-5} M and 10^{-4} M.

Microtubule sliding on doublet bundles was observed under a fluorescent microscope (Olympus, BX 60) with a 100× oil-immersion objective lens (Olympus PlanApo, NA=1.4) and recorded on videotape using a high-sensitivity silicon-intensified target camera (SIT camera, Hamamatsu Photonics, C2400-08) and a VHS videocassette recorder. To analyse the sliding velocity, the video images were traced by hand from the screen of a video monitor onto a sheet of transparent film. The sliding velocity was determined from the time measured by counting the number of video fields and the distance of microtubule movement measured on the traced images.

Electron microscopy

The axonemal fragments were resuspended in the reactivating solution containing 1 mM ATP (0.6 mM MgATP) and Ca^{2+} (10^{-4} M, 10^{-3} M or $<10^{-9}$ M) and incubated at 20°C for 5 minutes. After reactivation, the axonemes were digested with elastase (5 μg ml^{-1} elastase, Sigma type III and 5 μg ml^{-1} trypsin inhibitor, Sigma type I-S) for 7 minutes. To stop the digestion, glutaraldehyde was added to a final concentration of 2% on ice. After 15 minutes fixation at 10°C, the axonemes were pelleted by centrifugation at 28,000 *g* for 10 minutes at 4°C. The pelleted samples were fixed with 2% glutaraldehyde in the rinse buffer (0.15 M potassium acetate, 25 mM $MgSO_4$ and 10 mM phosphate buffer, pH 8.0) for 1 hour at 0°C. Then the samples were washed with the rinse buffer, postfixed in 1% OsO_4 in the rinse buffer for 45 minutes at 0°C, dehydrated in a graded ethanol series and embedded in Epon 812 (TAAB). Silver-gold sections were cut with a glass knife on Sorvall, MT2-B ultramicrotome, collected on copper grids, stained with uranyl acetate and lead citrate, and observed at 80 kV with a JEOL JEM100CX electron microscope.

When the sliding pattern of disintegrated axonemes was studied, we examined thicker bundles consisting of doublets and the central pair. We used the conventional numbering system for the doublets originally proposed by Afzelius (Afzelius, 1959). The doublet microtubules in the thicker bundles were identified from the position of the 5-6 bridge and the orientation of the central pair, but we could not identify all the doublets of the thinner bundles. The identification of microtubules in the thicker bundles based on the position of the 5-6 bridge and the orientation of the central pair would be appropriate, because the central pair of *P. depressus* flagella does not rotate with respect to the peripheral doublet microtubules (Takahashi et al., 1991). In order to identify the sliding pattern of thicker bundles, we photographed randomly selected cross sections of thicker bundles at a magnification of 50,000×. The photographs were labelled with code numbers and shuffled before the identification to avoid subjectivity in the judgement.

Results

Sliding disintegration of elastase-treated axonemes

ATP induced different patterns of sliding disintegration in the elastase-treated axonemes depending on its concentration. At a low concentration of ATP, such as 20 μM, the elastase-treated axonemes separated into a few groups of doublets or even into individual doublets as a result of more than two times (≥3) of sliding events, in which all sliding events were continuously induced (Fig. 1A and the left graph of Fig. 1C). (A sliding event is an ATP-induced, long-distance sliding that appears to occur between two adjacent doublets.) Similar sliding is observed in trypsin-treated axonemes (Summers and Gibbons, 1971), regardless of the ATP concentration. By contrast, at ATP concentrations higher than 0.1 mM, about half of the elastase-treated axonemes showed only one sliding events or two, so that the axonemes separated lengthwise into two or three bundles of doublets (Fig. 1B and the middle graph of Fig. 1C). The remaining half of the axonemes went through more than two sliding events, the first of which separated the axoneme into two bundles and the second and later sliding events occurred a few seconds after the first sliding. When the concentration of Ca^{2+} was increased to 10^{-4} M, the axonemes showing one or two sliding events at 1 mM ATP increased to more than 80%, dominated by those that were split into a pair of bundles as the result of only a single sliding event (right graph of Fig. 1C). These observations indicate a possibility that the activity of dynein arms is regulated by ATP and Ca^{2+}.

The effect of Ca^{2+} on the sliding velocity observed in the elastase-treated axonemes that slid into paired bundles at 1 mM ATP (0.6 mM MgATP) is summarized in Fig. 2. The average sliding velocities were 9.8±2.8 μm $second^{-1}$ (mean±s.d., n=45) and 9.2±2.5 μm $second^{-1}$ (n=53) at low ($<10^{-9}$ M) (Fig. 2A) and high (10^{-4} M) (Fig. 2B) concentrations of Ca^{2+}, respectively. The sliding velocities at low and high Ca^{2+} concentrations were not significantly different (P>0.2, Mann–Whitney U test). This seems to accord with previous reports that Ca^{2+} does not affect the sliding velocity in trypsin-treated axonemes (Walter and Satir, 1979; Mogami and Takahashi, 1983; Okagaki and Kamiya, 1986; Vale and Toyoshima, 1989). The following experiments, however, show that microtubule sliding in flagellar axonemes is regulated by Ca^{2+}. They also give us a clue to understanding why the velocity of sliding disintegration in the elastase-treated axonemes is apparently not affected by Ca^{2+}.

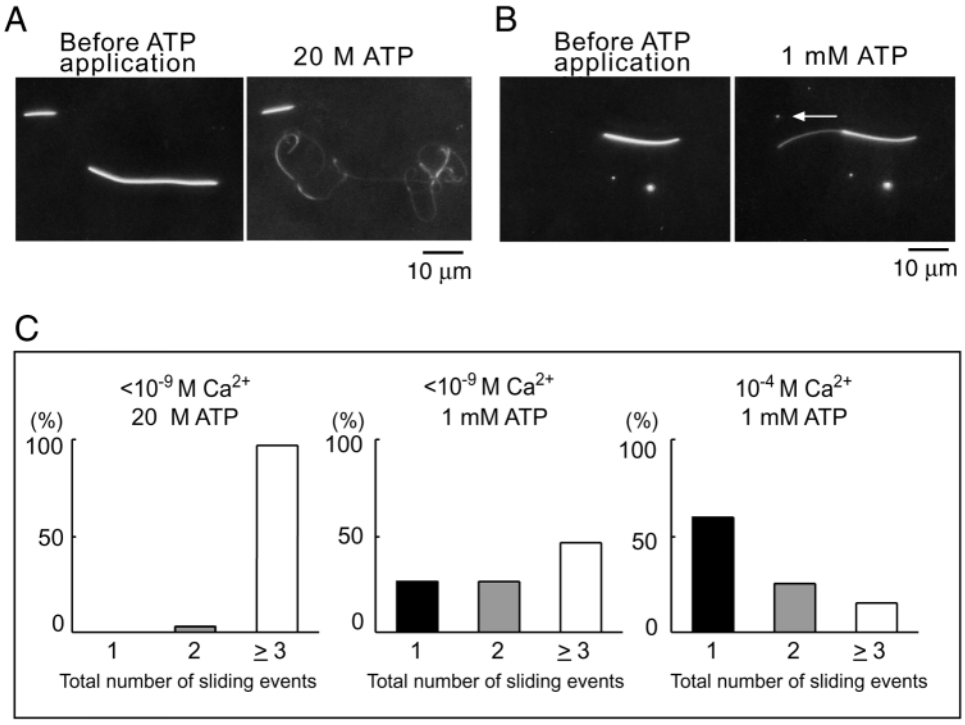

Fig. 1. (A,B) Elastase-treated axonemes before (left) and after (right) ATP application. 20 μM ATP at $<10^{-9}$ M Ca^{2+} induced more than two sliding events, causing sliding disintegration of axonemes into individual doublets (A), whereas 1 mM ATP at 10^{-4} M Ca^{2+} induced one sliding event that caused splitting of the axoneme into a pair of doublet bundles (B). The thinner bundle slid over the thicker bundle to the left (arrow in B). (C) Proportions of three types of sliding, categorized by the total number of sliding events (1, 2 and ≥3). Left, $<10^{-9}$ M Ca^{2+}, 20 μM ATP; middle, $<10^{-9}$ M Ca^{2+}, 1 mM ATP; right, 10^{-4} M Ca^{2+}, 1 mM ATP.

Splitting patterns of doublet bundles

When elastase-treated axonemes split into thinner and thicker bundles, the thickness of these bundles were clearly distinguished one from the other by dark-field microscopy, suggesting that the number of doublets in each of the two kinds of bundles are somewhat fixed. Electron microscopy of thin-sectioned bundles revealed that the thicker bundles consisted of five or six doublets and the central pair, whereas the thinner bundles consisted of four or fewer doublets and were without the central pair. Because the doublet microtubules do not rotate around the central pair in the species we used (Takahashi et al., 1991 for *Pseudocentrotus*; unpublished data for *Clypeaster*), we were able to identify each of the doublets in the thicker bundles from its position relative to the 5-6 bridge and the orientation of the central pair (Fig. 3A,B).

We recognized eight patterns of cross section among the bundles that contained the central pair. Of these, four patterns composed more than 90% of the bundles that were obtained at low concentrations of Ca^{2+} (Fig. 3C). For simplicity, we will hereafter call, for example, the cross-sectional pattern of a thicker bundle that contains the doublets 8, 9, 1, 2, 3 and the central pair a '8-3 pattern'. According to this convention, the four main patterns of thicker bundles obtained at $<10^{-9}$ M Ca^{2+} were 8-4, 8-3, 4-8 and 3-8 (Fig. 3A,B). The thinner bundles corresponding to the 8-4 and 8-3 patterns were assumed to consist of doublets 5-7 and 4-7, respectively (Fig. 3B). Lacking the central pair, they could be identified by the presence of the 5-6 bridge. The thinner bundles corresponding to the 4-8 and 3-8 patterns were assumed to be doublets 9-3 and 9-2, respectively. There were also bundles of three or four doublets that contained neither the 5-6 bridge nor the central pair. In these bundles, we could not identify the individual doublets.

The splitting pattern was affected by Ca^{2+}. As the concentration of Ca^{2+} increased, the frequency of 4-8 patterns gradually decreased so that at 10^{-6}-10^{-5} M Ca^{2+}, other three patterns (8-4, 8-3 and 3-8) were mainly observed. Similarly, at Ca^{2+} concentrations higher than 10^{-4} M, the frequency of 3-8 decreased so that at 10^{-3} M Ca^{2+}, we found mainly two patterns, 8-4 and 8-3. At Ca^{2+} concentrations lower than 10^{-7}

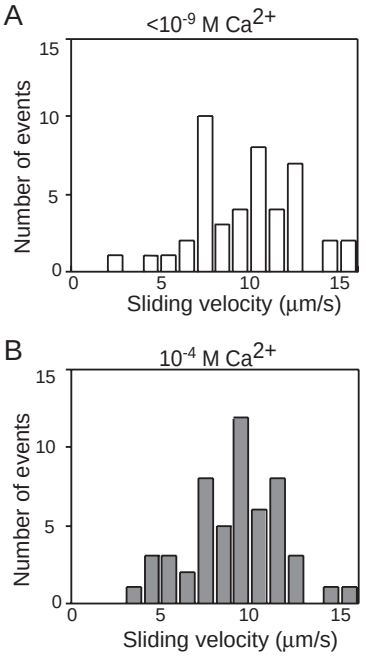

Fig. 2. Sliding velocities of elastase-treated axonemes at 1 mM ATP (0.6 mM MgATP). Distributions of the velocity at $<10^{-9}$ M Ca^{2+} (A) and 10^{-4} M Ca^{2+} (B) were similar to each other, and there was no significant difference between the two.

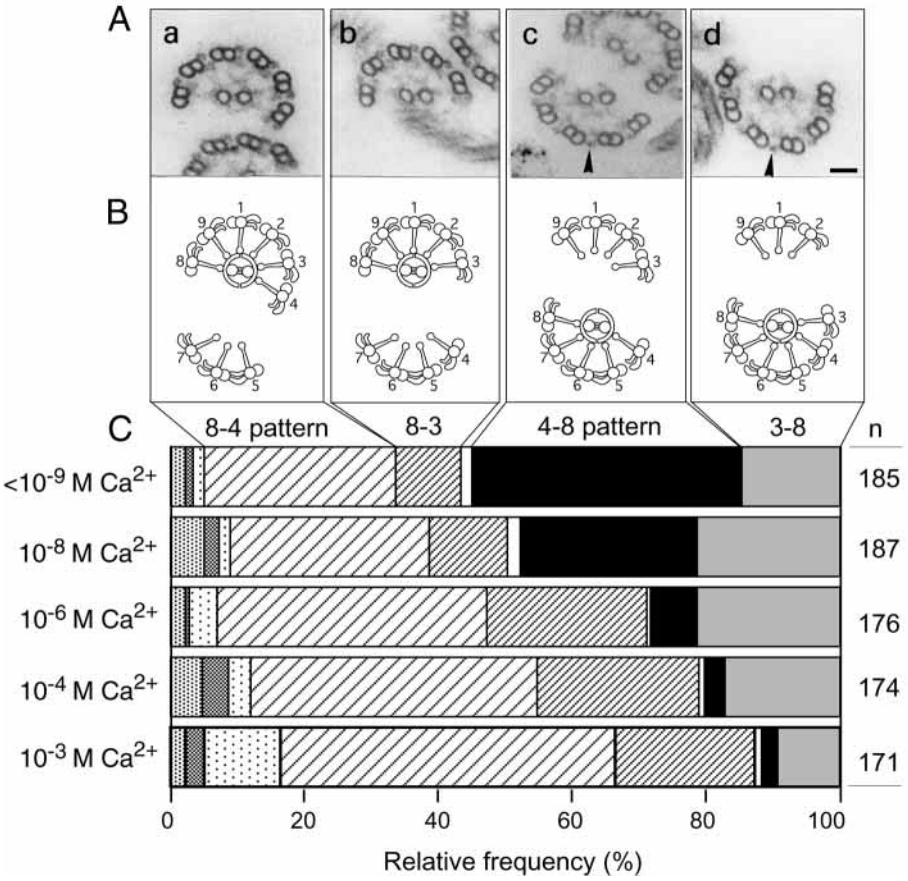

Fig. 3. Ultrastructural analysis of the effects of Ca^{2+} on four splitting patterns of the elastase-treated axonemes. (A) Electron micrographs showing the four patterns of the thicker bundles. Cross-sectional views of the axonemes are shown as seen from the base to the tip of the axonemes. Arrowheads in c and d indicate the 5-6 bridges. Scale bar, 50 nm. (B) Schematic diagrams of the thicker bundles corresponding to the electron micrographs shown in A with those of the thinner bundles obtained by the splitting. (C) Relative frequencies of eight splitting patterns of the doublet bundles that contained the central pair (CP) at $<10^{-9}$-10^{-3} M Ca^{2+}. Boxes from left to right for each concentration of Ca^{2+} indicate: one doublet with CP (grey boxes), 7-4 pattern (dark grey boxes), 7-3 pattern (dotted boxes), 8-4 pattern, 8-3 pattern, two doublets connected with a 5-6 bridge and with CP (open boxes), 4-8 pattern, and 3-8 pattern. Numbers (*n*) shown to the right of the columns are the numbers of cross-sections counted for each concentration of Ca^{2+}. Data obtained from three experiments were averaged because there was no significant difference in the pattern frequency.

M, the frequencies of 8-4 and 8-3 combined were about the same as those of 4-8 and 3-8 put together but, at 10^{-3} M Ca^{2+}, 8-4 plus 8-3 occurred more than seven times as frequently as did 4-8 plus 3-8 (Fig. 3C).

To induce the four patterns of thicker bundles, the dynein arms on the doublets 7, 3 and 2 of the thinner bundles and/or those on the doublets 3, 4 and 8 of the thicker bundles should be active during the sliding separation of the axonemes. To determine the doublets whose dynein arms were active, we examined the sliding direction of the thinner bundles with respect to the thicker bundles along which they slid, using elastase-treated axonemes that still had the sperm heads attached to them (Fig. 4). Demembranated sperm with the heads were placed on the glass surface of the perfusion chamber. Under a dark-field microscope, we cut each flagellum carefully into two or three short lengths using a glass microneedle without changing the orientation of the fragmented flagellum with respect to the head (Fig. 4, upper panel). When reactivating solution containing elastase, 1 mM ATP, and either 10^{-3} M or $<10^{-9}$ M Ca^{2+} was perfused, sliding disintegration of the fragments was induced as a bundle of doublets slid over the remaining part of the axoneme.

We found that, in most cases, the thinner bundles moved toward the head (or the thicker bundles moved away from the head) (Fig. 4, lower panel). Movements in this direction were observed in 84% of the axonemal fragments examined at $<10^{-9}$ M Ca^{2+} and this rate increased to 92% at 10^{-3} M Ca^{2+} (Table 1). Because the basal end of the axoneme is the 'minus', or more stable, end of the microtubule, and dynein is a minus-end-directed motor, the above observation indicates that the dynein arms on the thinner bundles were mainly active to induce the separation of the axonemes, regardless of the

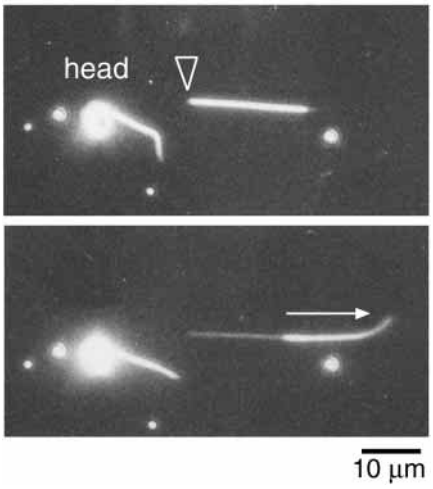

Fig. 4. Sliding of a thicker bundle over a thinner bundle in an elastase-treated flagellar axoneme with a head. Dark-field micrographs of a sperm flagellum before (top) and after (bottom) induced sliding. A flagellum was cut in two with a glass needle (arrowhead, top) and treated with elastase. Application of 1 mM ATP at 10^{-3} M Ca^{2+} induced lengthwise splitting into two bundles with the thicker bundle sliding to the right (bottom, arrow) (i.e. away from the head), leaving a thinner bundle attached to the glass surface.

Table 1. Proportions of thin and thick bundles that slide towards the basal end of the flagella at different Ca^{2+} concentrations

Ca^{2+}	Thinner bundles	Thicker bundles	Paired axonemal fragments
$<10^{-9}$ M	84.2%	15.8%	171
10^{-3} M	91.8%	8.2%	98

concentration of Ca^{2+}. We suggest that, at low concentrations of Ca^{2+}, the dynein arms on doublets 7, 3 and 2 of the thinner bundles are mainly active to induce the 8-4, 8-3, 4-8 and 3-8 patterns, and that, at high concentration of Ca^{2+} (10^{-3}-10^{-4} M), the dynein arms on doublet 7 of the thinner bundles are mainly active to induce the 8-4 and 8-3 patterns (Fig. 3). This implies that the activity of the dynein arms of the thicker bundles is inhibited.

Microtubule sliding on thinner and thicker bundles in an improved assay system

To understand the role of the central pair in the regulation of the dynein activity, we examined the effect of Ca^{2+} on microtubule sliding on bundles with or without the central pair. The thinner and thicker bundles were obtained from elastase-treated axonemes by application of 1 mM ATP in the presence of 10^{-4} M Ca^{2+}. When singlet microtubules were added to the split bundles, we observed sliding of the singlet microtubules not only on the thinner bundles but also on the thicker bundles at $<10^{-9}$ M-10^{-4} M Ca^{2+} (Fig. 5). This is apparently inconsistent with the above suggestion that the dynein arms on the thinner bundles are mainly active when the axonemes slid into two bundles (Table 1). To see what exactly happens, we analysed the behaviour of microtubules on the bundles.

Before describing the behaviour of microtubules, some improvements in our assay method should be realized. In the previous study (Yoshimura and Shingyoji, 1999), in which we developed the new sliding assay system, microtubule sliding was not always smooth. In the present study, we reduced the flow rate and kept a constant depth of the perfusion in order to maintain the activity of dynein arms that were exposed on the doublets. After these improvements, the behaviour of microtubules on the bundles changed. First, the number of bundles supporting active microtubule sliding increased (from 30% in the original method to >50% in the new method). Second, the back-and-forth movements of microtubules observed in the previous study were not observed in the present study, whereas a different type of back-and-forth movements was observed. Third, microtubules slid on thinner and thicker bundles at significantly different speeds in the previous study, but no such difference was found in the present study.

Frequency of microtubule sliding on thinner and thicker bundles

Fig. 6A summarizes the behaviour of microtubules attached on the thinner and thicker bundles. Because only one of the doublets of the bundles has dynein arms exposed (Fig. 3), orientations of doublet bundles on the glass surface are important to determine whether singlet microtubules are able to interact with the bundles. Thinner bundles showed straight and curved configuration, while thicker bundles were almost straight. The number of bundles to which microtubules attached and the number of microtubules attached to the bundles are shown in the right-hand column of Fig. 6A. The difference in configuration of bundles is probably related to the different numbers of thinner and thicker bundles to which microtubules attached. Comparison of the number of bundles with the number of microtubules, however, indicates that the

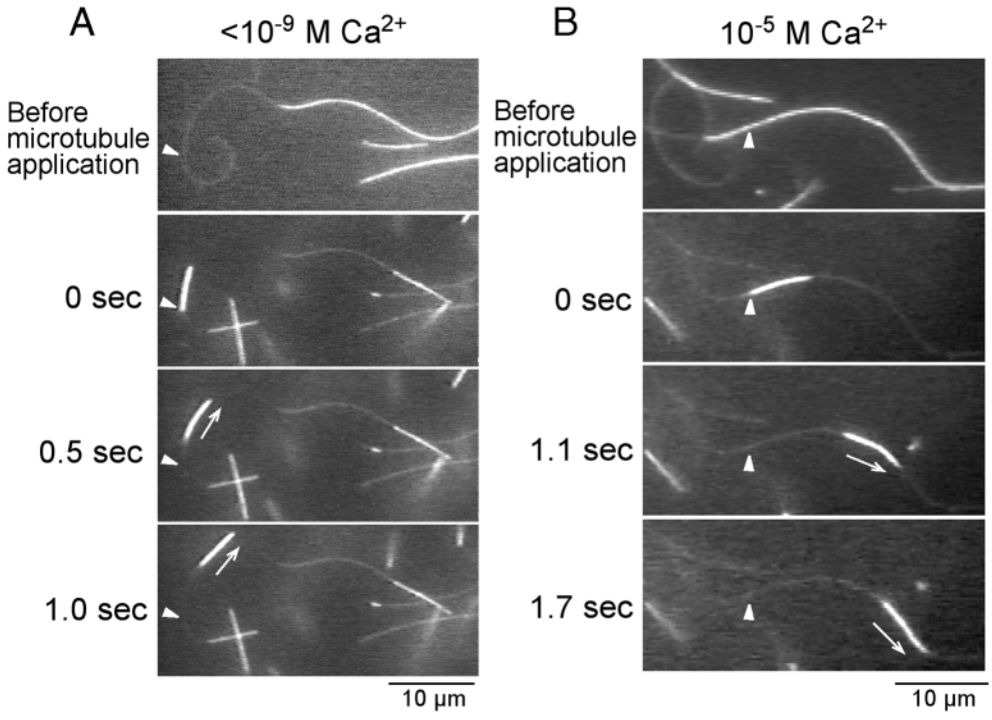

Fig. 5. Sliding of singlet microtubules along the thinner (A) and the thicker (B) bundles. (A) $<10^{-9}$ M Ca^{2+}. (B) 10^{-5} M Ca^{2+}. Similar sliding was observed both on the thinner and the thicker bundles regardless of the concentration of Ca^{2+}. The top panels in each case were recorded under stronger illumination to observe the paired bundles before singlet microtubules were added. The following three panels in each case, which were recorded under decreased illumination to record clearer image of singlet microtubules, are sequential images of the movements of singlet microtubules along the bundles. Arrowheads indicate the starting positions of the left ends of the singlet microtubules that interacted with the bundles (at 0 seconds). Arrows indicate the direction of sliding of the singlet microtubules.

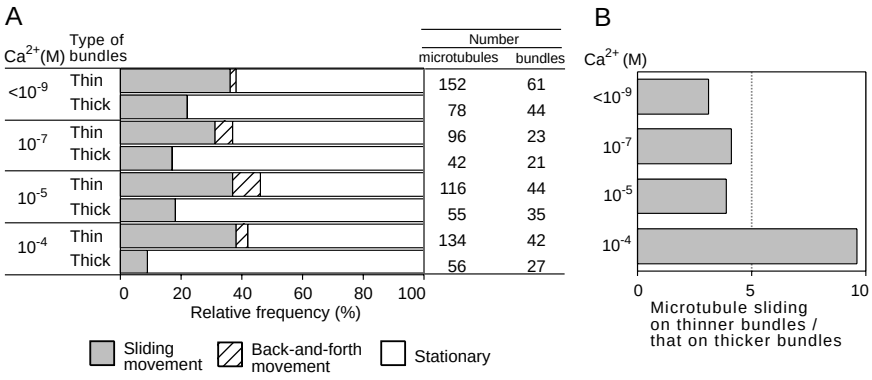

Fig. 6. (A) Behaviour of microtubules on thinner (Thin) and thicker (Thick) bundles at various concentrations of Ca^{2+}. The microtubules that attached to the bundles showed sliding movement (solid boxes), back-and-forth movement (hatched boxes) or no movement (open boxes). The numbers of bundles with which microtubules interacted are shown in the right-hand column. (B) The ratio of the number of occurrences of microtubule sliding on the thinner bundles to that on the thicker bundles at various concentrations of Ca^{2+}.

thicker bundles had lower affinity to microtubules than the thinner bundles. The frequency of microtubule sliding was about 30-40% on the thinner bundles but was less than 20% (at $<10^{-9}$-10^{-5} M Ca^{2+}) and 9% (at 10^{-4} M Ca^{2+}) on the thicker bundles. Fig. 6B shows ratio of the number of occurrences of microtubule sliding on the thinner bundles to that on the thicker bundles. At Ca^{2+} concentration $\leq 10^{-5}$ M, the ratio was about 4 but, at 10^{-4} M Ca^{2+}, it increased to 9.6, indicating that the sliding on the thicker bundles occurs one tenth as frequently as that on the thinner bundles in the presence of 10^{-4} M Ca^{2+}.

In the present improved sliding assay system, the microtubule sliding was smooth on both the thinner and the thicker bundles. But a back-and-forth movement with a distance of about 0.5-1 μm was observed only on curved regions along the thinner bundles at fewer than 10% of the microtubules attached to the bundles (hatched boxes in Fig. 6A). We need more detail analysis of the back-and-forth movement to know whether it is related to the regulation of dynein activity.

Velocity of microtubule sliding on thinner and thicker bundles

Most of the microtubules moved smoothly throughout the sliding, and this smooth movement was not changed by the presence of Ca^{2+} (Fig. 7). The time course of microtubule sliding on the thinner bundles and that on the thicker bundles was similar in the present assay system (Fig. 7A). An increase of Ca^{2+} concentration, however, affected the velocity of microtubule sliding on the thicker bundles (Fig. 7B).

Fig. 8 summarizes the velocity of microtubule sliding at 1 mM ATP (0.9 mM MgATP) on the thinner (left panels) and the thicker (right panels) bundles at lower (A) and higher (B) concentrations of Ca^{2+}. The sliding velocities did not show a Gaussian distribution but showed a broad distribution with a peak at around the middle and a longer tail towards higher sliding velocities (Fig. 8). At $<10^{-9}$ M Ca^{2+}, the distribution of sliding velocity was similar on the thinner and on the thicker bundles (Fig. 8A). At 10^{-7}-10^{-4} M Ca^{2+}, the distribution of the sliding velocities on the thinner bundles was also similar to that at low concentration of Ca^{2+}, whereas that on the thicker bundles shifted towards the lower velocities. Statistical differences between the sliding velocities on the thinner and the thicker bundles at $<10^{-9}$ and at 10^{-7}-10^{-4} M Ca^{2+} were examined by using the Mann–Whitney *U* test. We found that the sliding velocity on the thinner bundles and that on the thicker bundles were not different at low concentrations of Ca^{2+} but were significantly different in the presence of Ca^{2+} ($P<0.01$). At any Ca^{2+} concentration of 10^{-7}-10^{-4} M, the sliding velocity on the thicker bundles was lower than that on the thinner bundles. This showed clearly that the sliding velocity decreases with Ca^{2+} and the regulation of dynein activity by Ca^{2+} requires the presence of the central pair microtubules.

Discussion

The present study has shown that Ca^{2+} alters the dynein activity in the flagellar axoneme through a regulatory mechanism that involves the central-pair microtubules. We used a novel assay system that enabled us to analyse the sliding movements of a microtubule on a bundle of doublet microtubules with or

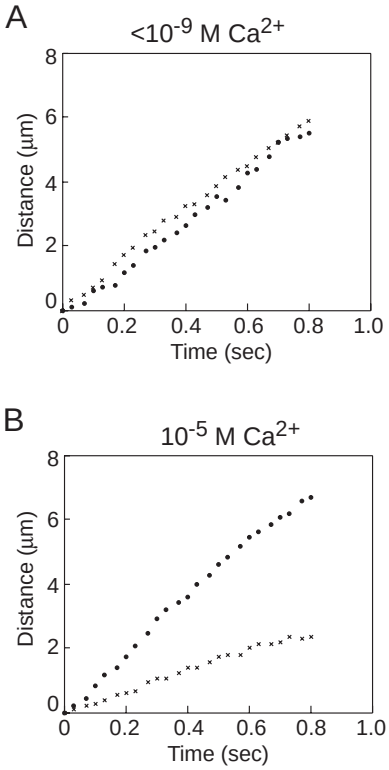

Fig. 7. Time courses of microtubule sliding movement at 1 mM ATP in the low (A) and high (B) concentrations of Ca^{2+}. The filled circles and crosses indicate the microtubules that slid along thinner and thicker bundles, respectively.

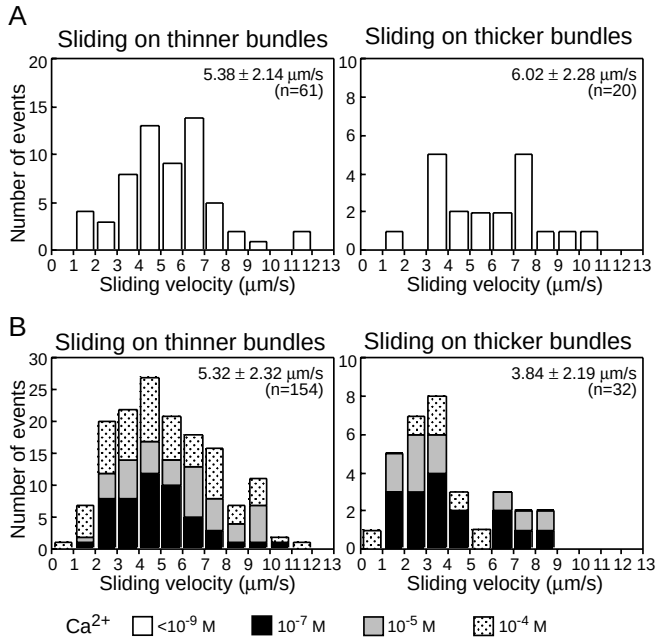

Fig. 8. Distribution of microtubule sliding velocities on thinner (left) and thicker (right) bundles at 1 mM ATP (0.9 mM MgATP) and low (A) and high (B) concentrations of Ca^{2+}. The sliding velocities are shown at $<10^{-9}$ M Ca^{2+}(open boxes), 10^{-7} M Ca^{2+} (filled boxes), 10^{-5} M Ca^{2+} (grey boxes) and 10^{-4} M Ca^{2+} (dotted boxes). Mean sliding velocities ± s.d. (*n*=number of microtubules) are shown in each graph. Velocities of sliding between the two doublet bundles (Fig. 2) were larger than those of microtubule sliding on bundles shown in this figure. This difference might be due to a different ionic strength between the reactivating solution (for Fig. 2) and the sliding assay buffer (for Fig. 8).

without the associated central pair. The doublet bundles were obtained by ATP-induced splitting of elastase-treated axonemes. We found that Ca^{2+} significantly decreased the velocity and the frequency of microtubule sliding on the thicker doublet bundles, which contained the central pair. Because the microtubule sliding on the thinner bundles without the central pair did not change by Ca^{2+}, we conclude that the regulation of dynein activity by Ca^{2+} depends directly on the central-pair microtubules. Thus, the elastase-treated axonemes allowed us to understand the activity of dynein arms under the regulatory mechanism involving the central pair (Shingyoji and Takahashi, 1995; Yoshimura and Shingyoji, 1999).

The Ca^{2+}-induced changes in the microtubule sliding velocity had not been demonstrated until our previous work using beating flagella (Bannai et al., 2000). In earlier studies, Ca^{2+} was shown to affect neither the sliding disintegration of axonemes treated with trypsin (~1 μg ml^{-1}) (Walter and Satir, 1979; Mogami and Takahashi, 1983; Okagaki and Kamiya, 1986) nor the gliding of microtubules on isolated axonemal dynein (Vale and Toyoshima, 1989). More recently, we found that trypsin digested some axonemal structures responsible for cyclical bending whereas elastase did not (Shingyoji and Takahashi, 1995). The present study using elastase-treated axonemes has demonstrated that the regulatory mechanism, which is necessary for cyclical bending and is retained in the elastase-treated axonemes, is also essential for the Ca^{2+} regulation of the microtubule-sliding activity of dynein. This regulatory mechanism requires the presence of the central-pair microtubules and the functional dynein arms that are attached to their natural location on the doublet. These results are consistent with the previous studies suggesting involvement of the central-pair microtubules in the Ca^{2+} regulation of flagellar bending movement (Sale, 1986; Bannai et al., 2000).

The present study has shown that Ca^{2+} causes three major changes in the dynein activity: (1) a decrease in the velocity of microtubule sliding on thicker bundles; (2) a decrease in the frequency of microtubule sliding on thicker bundles; and (3) changes in the splitting patterns of axonemes, which seem to correspond to the sites of active sliding among the axonemal microtubules. These changes were all closely associated with the presence of the central-pair microtubules but were induced at different concentrations of Ca^{2+}. This suggests that the three kinds of response to Ca^{2+} might be regulated by different mechanisms.

Our previous study has shown that trifluoperazine inhibits the 'quiescence' of sperm flagella, implying that Ca^{2+}-calmodulin is involved in the regulation of sliding that leads to the quiescence at 10^{-4} M Ca^{2+} (Bannai et al., 2000). The present study suggests that the quiescence is caused not only by the decrease in sliding frequency but also by the decrease in sliding velocity of dynein arms at one side (probably on doublet 3) of the central-pair microtubules. Smith (Smith, 2002b) has recently shown in *Chlamydomonas* flagella that the microtubule sliding velocity of axonemes lacking the central pair is reduced at $<10^{-8}$ M Ca^{2+} compared with that of the wild-type axonemes, but is restored by 10^{-4} M Ca^{2+}. She has also shown that calmodulin is involved in this Ca^{2+} regulation of microtubule sliding. This suggests a similar regulation of flagellar motility in both the sea urchin sperm and the *Chlamydomonas* flagella.

The patterns of splitting of the elastase-treated axonemes into two doublet bundles with or without the central pair are probably related to the mechanism regulating the dynein activity. We have found four main patterns of splitting, and the frequency of their appearance depended on the Ca^{2+} concentration. The four patterns were the thicker bundles consisting of the 8-4, 8-3, 4-8 and 3-8 doublet groups, with their corresponding thinner bundles of the remaining four or three doublets. Spontaneous axonemal fracture into a thinner and a thicker bundle has previously been reported in the quiescent sea urchin sperm flagella at high Ca^{2+} concentrations, in which the 8-3 pattern of the thicker bundles was dominant (Sale, 1986). Holwill and Satir (Holwill and Satir, 1994) have developed a physical model of axonemal splitting based on the observation of splitting of the axonemes, including six-and-three doublet groups and five-and-four doublet groups. This model provides a physical basis for the axonemal splitting that was observed in the present study.

Our analysis of the splitting patterns provided some interesting findings. The dynein arms on the thinner bundles, but not those on the thicker bundles, were active to produce microtubule sliding and to split the axonemes into paired bundles. Furthermore, we found that the occurrence of the 8-4 and 8-3 patterns and of the 4-8 and 3-8 patterns were similar at lower concentrations of Ca^{2+}, whereas the 8-4 and 8-3 patterns increased and the 4-8 and 3-8 patterns decreased with an increase of the Ca^{2+} concentration. These changes in the frequency of occurrence might be related to the waveforms of

reactivated flagella: the flagellar beating is nearly symmetrical at lower concentrations of Ca^{2+}, becoming increasingly asymmetrical with an increase of Ca^{2+} and finally becomes quiescent with a large principal bend at the base of the flagella at $\geq 10^{-4}$ M Ca^{2+}. The increase in asymmetry and the quiescence are induced by the inhibition of reverse-bend formation (Brokaw, 1979; Gibbons and Gibbons, 1980; Bannai et al., 2000). Thus, it is likely that the occurrence of the 4-8 and 3-8 patterns, which decreases with Ca^{2+} concentration, is related to the reverse-bend formation. If this is the case, switching between the group of the 8-4 and 8-3 patterns and the group of the 4-8 and 3-8 patterns – in other words, switching of the activity of dynein arms between doublet 7 (of thinner bundles) and doublet 3 or 2 (of the thinner bundles) – would be the basis for the alternate formation of the principal and the reverse bends.

The mechanism regulating the dynein activity to split the axoneme into a thinner and a thicker bundle has been unclear. From the present result, we can speculate about the roles of the two microtubules of the central pair. Structural and biochemical differences between the C1 and C2 microtubules with their associated projections have been described in *Chlamydomonas* flagella, suggesting possible different roles of C1 and C2 in the regulatory mechanism (Smith and Lefebvre, 1997; Mitchell and Sale, 1999; Porter and Sale, 2000; Smith, 2002a). In sea urchin sperm flagella, two microtubules of the central pair and their associated projections look similar in electron micrographs, and their biochemical and physiological differences have not been well documented. If we assume that the microtubules that are near doublets 7 and 3 are C1 and C2, respectively, similar to those of *Chlamydomonas*, the alternate activation of dynein might be regulated through the radial spokes by some signal from C1 and C2. The signal might be associated with a protein phosphorylation (Yang et al., 2000; Roush-Gaillard et al., 2001), with Ca^{2+}-calmodulin (Bannai et al., 2000; Smith, 2002b) or with changes in the mechanical states (Omoto et al., 1999; Bannai et al., 2000).

The elastase-treated axonemes showed different sliding features with varying ATP concentration. Low concentrations of ATP induced sliding disintegration of the axonemes into individual doublets, indicating that the dynein arms on any doublet of the axonemes are active. By contrast, high concentrations of ATP induced splitting of the axonemes into two or three bundles, indicating that the dynein arms attached to the doublets (3 or 7) near the central pair are active but those on the remaining doublets are inactive. These observations show that the dynein activity is inhibited at high concentrations of ATP but that the inhibition is overridden by the CP/RS. The inhibitory effect of a physiological concentration of ATP on the number of doublets that slide has been demonstrated in *Tetrahymena* cilia by Kinoshita et al. (Kinoshita et al., 1995), although, in their study, the sliding was also inhibited at low concentration of ATP, which is different from the present finding. Similar inhibition of the outer arms by a high level of ATP has also been reported in CP/RS-deficient *Chlamydomonas* mutants, in which lower concentrations of ATP induce beating of paralysed flagella (Omoto et al., 1996). The CP/RS complex is thought to override the ATP inhibition by activating the inner arms in a coordinated fashion in *Chlamydomonas* (Porter and Sale, 2000). The roles of ATP concentrations in the mechanism regulating the dynein activity might be similar in cilia and flagella of different species and the CP/RS might release the inhibitory effect of high ATP concentrations (Bannai et al., 2000).

The role of the CP/RS in the Ca^{2+} regulation of dynein activity also depends on the ATP concentration. At low concentrations of ATP, the axonemes of the CP/RS-deficient *Chlamydomonas* mutants are able to beat and show Ca^{2+}-dependent waveform conversion (Wakabayashi et al., 1997). At a high (physiological) level of ATP, however, the CP/RS is suggested to play a key role in the Ca^{2+} regulation of waveform and microtubule sliding (Hosokawa and Miki-Noumura, 1987; Smith, 2002b). The present result in sea urchin sperm flagella show that the CP/RS is essential for the Ca^{2+} regulation of dynein activity at the physiological level of ATP.

We thus conclude that the outer and probably also the inner dynein arms are inhibited by physiological levels of ATP and that the CP/RS complex might override the inhibition by activating both the outer and inner dynein arms. When the CP/RS complex is functional, both the C1 and C2 microtubules might alternately activate the dynein arms on the near microtubules. We also postulate that mechanism regulating the activity of dynein by C2 is sensitive to Ca^{2+}.

Finally, we discuss the velocity of sliding of the elastase-treated axonemes to induce thicker and thinner bundles. The velocity of sliding disintegration was not affected by Ca^{2+} even in the elastase-treated axonemes. This is apparently inconsistent with the Ca^{2+}-induced inhibition of dynein activity on the thicker bundles that was shown in the novel sliding assay. This inconsistency could be explained, however, if we take all results of the present study into consideration. When the elastase-treated axonemes split lengthwise into two bundles, the dynein arms on the thinner bundles are predominantly active at low as well as at high concentrations of Ca^{2+}. This means that the velocity of sliding induced by dynein arms on the thicker bundles could not be measured in the sliding disintegration. Our study also showed that the velocity and the frequency of sliding of singlet microtubules that interacted with the dynein arms exposed on the thicker bundles, but not with those on the thinner bundles, were significantly inhibited by Ca^{2+}. Ca^{2+} inhibited the activity of the dynein arms on the thicker bundles but not that on the thinner bundles, and the activity of dynein arms on the thinner bundles was required for the sliding disintegration. Thus, it is very plausible that the inhibitory effect of Ca^{2+} could not be detected in the sliding disintegration of the axonemes.

We would like to express our gratitude to Professor Keiichi Takahashi for his kind guidance, encouragement throughout the study and reading the manuscript. We thank the director and staff of Misaki Marine Biological Station (University of Tokyo) for providing sea urchins. This work was supported by grants from Takeda Science Foundation, Hayashi Memorial Foundation for Female Natural Scientists and Grant-in-Aid for Scientific Research from the Japan Society for the Promotion of Science (to C.S.).

References

Afzelius, B. A. (1959). Electron microscopy of the sperm tail. Results obtained with a new fixative. *J. Biophys. Biochem. Cytol.*, **5**, 269-278.

Bannai, H., Yoshimura, M., Takahashi, K. and Shingyoji, C. (2000). Calcium regulation of microtubule sliding in reactivated sea urchin sperm flagella. *J. Cell Sci.*, **113**, 831-839.

Bessen, M., Fay, R. B. and Witman, G. B. (1980). Calcium control of

waveform in isolated flagellar axonemes of *Chlamydomonas*. *J. Cell Biol.* **86**, 446-455.

Brokaw, C. J. (1979). Calcium-induced asymmetrical beating of Triton-demembranated sea urchin sperm flagella. *J. Cell Biol.* **82**, 401-411.

Brokaw, C. J. (1980). Elastase digestion of demembranated sperm flagella. *Science.* **207**, 1365-1367.

Gibbons, B. H. and Gibbons, I. R. (1980). Calcium-induced quiescence in reactivated sea urchin sperm. *J. Cell Biol.* **84**, 13-27.

Gibbons, I. R., Shingyoji, C., Murakami, A. and Takahashi, K. (1987). Spontaneous recovery after experimental manipulation of the plane of beat in sperm flagella. *Nature* **325**, 351-352.

Goldstein, D. A. (1979). Calculation of the concentration of free cations and cation-ligand complexes in solution containing multiple divalent cations and ligands. *Biophys. J.* **26**, 235-242.

Holwill, M. E. J. and McGregor, J. L. (1976). Effects of calcium on flagellar movement in the trypanosome *Crithidia oncopelti*. *J. Exp. Biol.* **65**, 229-242.

Holwill, M. E. J. and Satir, P. (1994). Physical model of axonemal splitting. *Cell Motil. Cytoskel.* **27**, 287-298.

Hosokawa, Y. and Miki-Noumura, T. (1987). Bending motion of *Chlamydomonas* axonemes after extrusion of central-pair microtubules. *J. Cell Biol.* **105**, 1297-1301.

Hyams, J. S. and Borisy, G. G. (1978). Isolated flagellar apparatus of *Chlamydomonas*: characterization of forward swimming and alteration of waveform and reversal of motion by calcium ions in vitro. *J. Cell Sci.* **33**, 235-253.

Izumi, A. and Miki-Noumura, T. (1985). *Tetrahymena* cell model exhibiting Ca-dependent behavior. *Cell Motil.* **5**, 323-331.

Kamiya, R. (2002). Functional diversity of axonemal dyneins as studied in *Chlamydomonas* mutants. *Int. Rev. Cytol.* **219**, 115-155.

Kinoshita, S., Miki-Noumura, T. and Omoto, C. K. (1995). Regulatory role of nucleotides in axonemal function. *Cell Motil. Cytoskel.* **32**, 46-54.

Mitchell, D. R. and Sale, W. S. (1999). Characterization of a *Chlamydomonas* insertional mutant that disrupts flagellar central pair microtubule-associated structures. *J. Cell Biol.* **144**, 293-304.

Mogami, Y. and Takahashi, K. (1983). Calcium and microtubule sliding in ciliary axonemes isolated from *Paramecium caudatum*. *J. Cell. Sci.* **61**, 107-121.

Naitoh, Y. and Kaneko, H. (1972). Reactivated Triton-extracted models of *Paramecium*: modification of ciliary movement by calcium ions. *Science* **176**, 523-524.

Okagaki, T. and Kamiya, R. (1986). Microtubule sliding in mutant *Chlamydomonas* axonemes devoid of outer or inner dynein arms. *J. Cell Biol.* **103**, 1895-1902.

Omoto, C. K. and Brokaw, C. J. (1985). Bending patterns of *Chlamydomonas* flagella: II. Calcium effects on reactivated *Chlamydomonas* flagella. *Cell Motil.* **5**, 53-60.

Omoto, C. K., Yagi, T., Kurimoto, E. and Kamiya, R. (1996). Ability of paralyzed flagella mutants of *Chlamydomonas* to move. *Cell Motil. Cytoskel.* **33**, 88-94.

Omoto, C. K., Gibbons, I. R., Kamiya, R., Shingyoji, C., Takahashi, K. and Witman, G. B. (1999). Rotation of the central pair microtubules in eukaryotic flagella. *Mol. Biol. Cell* **10**, 1-4.

Porter, M. E. and Sale, W. S. (2000). The 9+2 axoneme anchors multiple inner arm dyneins and a network of kinase and phosphatases that control motility. *J. Cell Biol.* **151**, F37-F42.

Roush-Gaillard, A., Diener, D. R., Rosenbaum, J. L. and Sale, W. S. (2001). Flagellar radial spoke protein 3 is an A-kinase anchoring protein (AKAP). *J. Cell Biol.* **153**, 443-448.

Sale, W. S. (1986). The axonemal axis and Ca^{2+}-induced asymmetry of active microtubule sliding in sea urchin sperm tails. *J. Cell Biol.* **102**, 2042-2052.

Shingyoji, C. and Takahashi, K. (1995). Cyclical bending movements induced locally by successive iontophoretic application of ATP to an elastase-treated flagellar axoneme. *J. Cell. Sci.* **108**, 1359-1369.

Shingyoji, C., Higuchi, H., Yoshimura, M., Katayama, E. and Yanagida, T. (1998). Dynein arms are oscillating force generators. *Nature* **393**, 711-714.

Smith, E. F. (2002a). Regulation of flagellar dynein by the axonemal central apparatus. *Cell Motil. Cytoskel.* **52**, 33-42.

Smith, E. F. (2002b). Regulation of flagellar dynein by calcium and a role for an axonemal calmodulin and calmodulin-dependent kinase. *Mol. BIol. Cell* **13**, 3303-3313.

Smith, E. F. and Lefebvre, P. A. (1997). The role of central apparatus components in flagellar motility and microtubule assembly. *Cell Motil. Cytoskel.* **38**, 1-8.

Summers, K. E. and Gibbons, I. R. (1971). Adenosine triphosphate-induced sliding of tubules in trypsin-treated flagella of sea-urchin sperm. *Proc. Natl. Acad. Sci. USA* **68**, 3092-3096.

Takahashi, K., Shingyoji, C. and Kamimura, S. (1982). Microtubule sliding in reactivated flagella. *Symp. Soc. Exp. Biol.* **35**, 159-177

Takahashi, K., Shingyoji, C., Katada, J., Eshel, D. and Gibbons, I. R. (1991). Polarity in spontaneous unwinding after prior rotation of the flagellar beat plane in sea-urchin spermatozoa. *J. Cell Sci.* **98**, 183-189.

Vale, R. D. and Toyoshima, Y. Y. (1989). Microtubule translocation properties of intact and proteolytically digested dyneins from *Tetrahymena* cilia. *J. Cell Biol.* **108**, 2327-2334.

Wakabayashi, K., Yagi, T. and Kamiya, R. (1997). Ca^{2+}-dependent waveform conversion in the flagellar axoneme of *Chlamydomonas* mutants lacking the central-pair/radial spoke system. *Cell Motil. Cytoskel.* **38**, 22-28.

Walter, M. F. and Satir, P. (1979). Calcium does not inhibit active sliding of microtubules from mussel gill cilia. *Nature* **278**, 69-70.

Witman, G. B., Plummer, J. and Sander, G. (1978). *Chlamydomonas* flagellar mutants lacking radial spokes and central tubules. *J. Cell Biol.* **76**, 729-747.

Yang, P., Fox, L., Colbran, R. J. and Sale, W. S. (2000). Protein phosphatases PP1 and PP2A are located in distinct positions in the *Chlamydomonas* flagellar axoneme. *J. Cell Sci.* **113**, 91-102.

Yoshimura, M. and Shingyoji, C. (1999). Effects of the central pair apparatus on microtubule sliding velocity in sea urchin sperm flagella. *Cell Struct. Funct.* **24**, 43-54.